HHS Public Access

Author manuscript

J Org Chem. Author manuscript; available in PMC 2023 December 05.

Published in final edited form as:

J Org Chem. 2023 September 15; 88(18): 13135–13141. doi:10.1021/acs.joc.3c01362.

Synthesis of Neocannabinoids Using Controlled Friedel-Crafts Reactions

Alexandra M. Millimaci,

Richard V. Trilles,

James McNeely,

Lauren E. Brown,

Aaron B. Beeler[*], **John A. Porco Jr.**[*]

Department of Chemistry, Boston University, Boston, Massachusetts 02215, United States

Abstract

A one-step transformation to produce 8,9-dihydrocannabidiol (H_2CBD) and related "neocannabinoids" *via* controlled Friedel-Crafts reactions is reported. Experimental and computational studies probing the mechanism of neocannabinoid synthesis from cyclic allylic alcohol and substituted resorcinol reaction partners provide understanding of the kinetic and thermodynamic factors driving regioselectivity for the reaction. Herein, we present a reaction scope for neocannabinoid synthesis including the production of both normal and abnormal isomers under both kinetic and thermodynamic control. Discovery and optimization of this one-step protocol between various allylic alcohols and resorcinol derivatives is discussed and supported with density-functional theory (DFT) calculations.

Graphical Abstract

[*]**Corresponding Authors** porco@bu.edu **(J.A.P, Jr.)**; beelera@bu.edu (A.B.B).

Author Contributions

The manuscript was written through contributions of all authors. All authors have given approval to the final version of the manuscript.

The authors declare the following competing financial interest(s): J.A.P, Jr. A.B, A. M., R.T., J.M., and L.E.B are inventors on a provisional patent application describing the synthesis of neocannabinoid isomers.

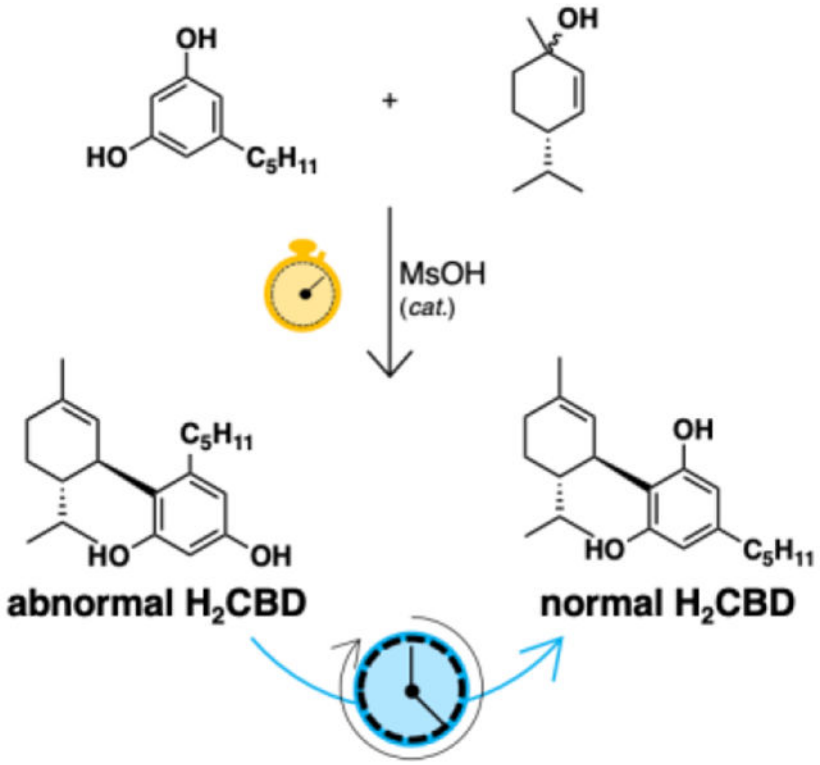

INTRODUCTION

Cannabidiol (CBD) **1** (Figure 1) was discovered in 1940 and is one of more than 100 identified cannabinoids in cannabis plants; together, CBD and tetrahydrocannabinol (THC) **2** account for almost half of the plant–s extract.[1,2] Although CBD has shown promise in therapeutic uses for Alzheimer's disease,[3] Parkinson's disease,[3] epilepsy,[3] and cancer,[3] its propensity for intramolecular cyclization to generate the psychoactive and DEA Schedule I-controlled substance THC **2** have limited its utility and potential.[4,5] Furthermore, marketing of CBD for consumption carries the risk of illicit use in the production of THC analogues in analogy to challenges associated with pseudoephedrine-to-methamphetamine.[6,7] These concerns have highlighted the potential of the synthetic cannabinoid 8,9-dihydrocannabidiol (H_2CBD) **3** to abrogate these concerns due to saturation of the exocyclic isoprene moiety, thereby preventing electrophilic cyclization to THC.[6] Thus, H_2CBD poses no legal issues as it is fully synthetic, can be scaled up from readily available starting materials that do not require cultivation of cannabis or hemp, and poses no concern for the generation of THC. Such molecules could provide a path toward cannabinoid-based therapeutics without psychotropic effects to prevent drug abuse liabilities.

In parallel studies involving CBD and abnormal cannabidiol **4** (Abn-CBD) it was found that their affinities for CB_1 and CB_2 receptors were substantially different.[8,9] It was then discovered that Abn-CBD and synthetic analogs (*e.g.* **5**, O-1602) have binding affinities to the orphaned cannabinoid receptors GPR18 and GPR55, two receptors which are responsible for effects of cannabinoids independent of CB_1 and CB_2.[9] Abnormal CBD **4**

is a CBD regioisomer in which the terpene subunit is positioned *ortho* to the *n*-pentyl substituent (*vs.* the *para* relationship present in "normal" CBD **1**), a structural difference for binding to other targets in future analogs. Further structure-activity relationship (SAR) studies show that the substitution of the alkyl chain from Abn-CBD, the relative position of aromatic groups, and sites with the ability to form hydrogen-bonds are important for binding to GPR18 and GPR55.[9,10] These findings suggest that synthetic investigations towards unnatural cannabinoid derivatives, herein referred to as "neocannabinoids," including abnormal H_2CBD **6** can greatly benefit therapeutic applications.[11,13]

A number of routes for the chemical synthesis of CBD and related molecules have been devised (Scheme 1).[14-17] The most efficient approach leverages Friedel-Crafts alkylation of olivetol **7** and chiral allylic alcohols such as menthadienol **8** under mild acidic conditions affording CBD through an S_N1' mechanism (Scheme 1A).[15,18] These reactions typically deliver exclusive diastereoselectivity wherein the olivetol substituent favors a *trans* orientation relative to the isopropyl group. Notably these reactions generally lack regioselectivity between the ("abnormal") **4** and ("normal") **1** isomers. Production of the generally undesired abnormal CBD isomer is often a complication in the synthetic production of CBD *via* the Friedel-Crafts route and can be further complicated by unwanted cycloetherification when using Brønsted acid catalysis. To address this issue, Baek and coworkers reported the synthesis of CBD **1** in 56% isolated yield along with 14% abnormal CBD isomer **4** using BF_3•OEt_2 on alumina (Al_2O_3) as a Lewis acid promoter.[15,19] Other modes of entry to synthetic CBD include the use of olivetol derivatives to control the site of reaction by removable "blocking group" strategies (*e.g.* ester or halogens), thereby inhibiting abnormal product formation.[15] This method, which mimics the biosynthesis of CBD, generally involves multiple synthetic steps to access CBD in good yields.[5]

The challenge in controlling regioselectivity of CBD synthesis without cyclization to THC birthed the expansion into the synthesis of relevant analogs. The racemic, reduced version of CBD (H_2CBD) **3** displays similar pharmacological properties to CBD and does not require chiral pool starting materials making it a promising synthetic target. Importantly, synthetic generation of H_2CBD provides room for reaction manipulation and optimization to control regioselectivity without the concern of unintended THC production. This prompted our efforts to develop a better understanding of the kinetic and thermodynamic factors that dictate regioselectivity in this reaction.

Herein, we describe our efforts toward an efficient and regioselective synthesis of normal and abnormal neocannabinoids. In this study, we confirmed that regioselectivity is largely controlled by both kinetic and thermodynamic considerations. Our findings were aligned with computational studies, thereby providing a model for a range of reaction partners and product distributions.

RESULTS AND DISCUSSION

We began our investigation by screening numerous Lewis and Brønsted acids to initiate allylic cation chemistry by mimicking the effects of BF_3•OEt_2 as reported in the literature.[20-22] Previously, Mascal and coworkers obtained normal CBD **3** in 71% yield

by *para*-toluenesulfonic acid (*p*-TsOH) acid-catalyzed addition to α-phellandrene **9** (Scheme 1B).[6,15] In an effort to match this efficiency, we considered the well-established Friedel-Crafts alkylation/cationic pathway using olivetol **7** and allylic alcohol **10** to access H_2CBD isomers **3** and **6** (Scheme 1C-D). Our catalyst scope included various Lewis acids including Sc(III)-, La(III)-, Eu(III)-, Yb(III)- triflates, *p*-TsOH and methanesulfonic acid (MsOH), as well as combinations of both Lewis and Brønsted acids. Metal triflates were tested over multiple time points with varying catalyst loadings and temperatures. All conditions screened provided a mixture of normal H_2CBD **3** and abnormal H_2CBD **6** (Table 1); in many cases, the *bis*-addition product **11** was also observed; reactions conducted at higher temperatures (40 °C) provided only cyclized products.[23-25] La(III)- and Yb(III)- triflates provided the highest conversion to H_2CBD **3** after 24 h, but also led to increased production of *bis*-addition product **11** which was ultimately a significant drawback for use of metal triflates. *p*-TsOH and MsOH both performed well in the reaction and optimally in CH_2Cl_2, although use of *p*-TsOH led to solubility issues. Thus, optimal reaction conditions were found using MsOH as catalyst. The friendliness of MsOH as a liquid with low corrosivity and toxicity in comparison to the other Brønsted acids made it very easy to work with.[26]

The MsOH-catalyzed reaction was optimized by evaluating catalyst loading, temperature, and time. In these studies, we found that initially the reaction generated roughly a 1:1 ratio of normal H_2CBD **3** to abnormal derivative **6** as well as *bis*-addition product **11** as a side product. However, we observed greater conversion to H_2CBD as determined by ^{1}H NMR analysis at a 24 h reaction time. Allowing the reaction to proceed beyond 24 h increased the amount of cycloetherification product **12**; accordingly, optimal reaction conditions to generate H_2CBD were 0.1 equiv. of MsOH at room temperature for 24 h (Table 1, entry 6). However, we believed that the apparent conversion from abnormal to normal isomers suggested that production of **6** could be a kinetic process and by terminating the reaction at an earlier timepoint, we could increase selectivity. Indeed, we were able to obtain abnormal H_2CBD 6 (rr = 1:1) in 41% isolated yield after 1 h reaction time (Table 1, entry 5), in contrast to an 81% isolated yield of normal H_2CBD **3** after 24 h.

We next tested the abnormal to normal equilibration hypothesis with a time study by treating pure abnormal isomer **6** with catalytic amounts of MsOH in CH_2Cl_2. We observed that the abnormal product does in fact equilibrate to the normal isomer **3** in as quickly as 1 h, with full consumption of **6** observed over a longer time period albeit with concomitant emergence of byproducts **11** and **12** (Table 2). Further screening was also conducted with *p*-TsOH and camphorsulfonic acid (CSA) as catalysts (*not shown*), but these acids exhibited poor solubility in CH_2Cl_2 and produced greater amounts of side products. Previous work by Crombie and coworkers showed that reactions of olivetol with electrophiles such as (+)-*trans*-car-2-ene epoxide[25] and **9**[27] in the presence of *p*-TsOH also afforded both abnormal and normal cannabinoids at early timepoints, with an “interconversion” of abnormal to normal occurring with elevated temperatures.[28] Consistent with our findings, it was noted that in this process the presumably kinetically favored abnormal cannabinoid transforms to the more thermodynamically stable normal cannabinoid.[27]

Further probing of a potential dissociative equilibration process was performed in a crossover experiment to refine mechanistic understanding. The experiment shown in Scheme

2 was designed using two different abnormal cannabinoids, **6** and **13**, which were treated under the same acidic conditions. Abnormal cannabinoid isomer **13** was prepared using divarinol and 1-methylcyclohex-2-en-1-ol as reaction partners. In this experiment, we expected equilibration from abnormal to normal cannabinoid *e.g.* **6** to **3** and **13** to **14**, as well as crossover products **15** and **16**, assuming that equilibration proceeds by disassociation to regenerate the allylic cation and resorcinol partner (Scheme 3). Using a combination of *in situ* ^{1}H NMR and HPLC-ELSD/MS analysis, we monitored the ratios of the pure abnormal cannabinoids **6/13**, their corresponding normal isomers **3/14**, and expected crossover products **15/16** (Scheme 2). As expected, we observed products **3** and **14** after 1 h, with only trace amounts of **15** and **16** detected; after 24 h, we obtained a considerable amount (26%) of crossover products.[29] Overall, this data confirmed that the generation of **3** from **6** (*cf.* Table 2) likely proceeds *via* an intermolecular retro-Friedel Crafts/Friedel-Crafts process[30] and not an intramolecular rearrangement pathway.

We next sought to prepare a small library of allylic alcohols for neocannabinoid synthesis. We envisioned a scope of allylic alcohols varying in substituents at the 4-position to determine the steric effects of normal *vs.* abnormal addition in terms of both kinetic and thermodynamic control. Five reagents (**10-10f**) were chosen to represent a gradual increase in sterics progressing from no substituents (**10c**) to the bulky *tert*-butyl substituted partner (**10f**). Likewise, selection of the resorcinol reagent also varied in both sterics and alkyl chain length. We chose orcinol (**7a**), olivetol (**7**), and 5-(1,1-dimethylheptyl) resorcinol (**7b**) as three reaction partners as shown in Table 3.

For all reagent pairings, we tracked the ratio of isomers generated at both 1 and 24 h by both HPLC and ^{1}H NMR analyses. We found that in almost all cases employing orcinol **7a** (Table 3, entries 1-4), the abnormal neocannabinoid **6ac-6a** was enriched within the first hour. The *tert*-butyl allylic alcohol (**10f**, Table 3, entry 5) was the only example where the normal neocannabinoid (**3af**) was the major product at the 1 h timepoint. The kinetic preference for the abnormal isomers can also be attributed to favorable electrostatics (Lowdin charges) between the *ortho* (relative to the resorcinol alkyl chain) carbons and the cationic partner as compared to the *para* carbons (see Figure S1 in the Supporting Information). Overall, we observed that the ratio of normal:abnormal (**3ac-3af:6ac-6af**) increases over time, consistent with our observation of a thermodynamic equilibration process. In order to rationalize these outcomes, the systems were studied computationally (Orca, r^{2}SCAN-3C/CPCM(CH_2Cl_2))[31-35] to understand the kinetic and thermodynamic factors driving the 1 h/24 h ratios observed (Table 3 and Supporting Information). Indeed, our calculations generally support the premise that with increasing bulk at the 4-position of the allylic alcohol partner, the normal product is increasingly thermodynamically favored (ΔG in Table 3), a likely consequence of the added steric strain introduced between the R_2/R_3 substituents and the R_1 sidechain. The computations suggest a kinetic preference for the abnormal isomer in **3(6)ac-3(6)ae** and **3(6)af** with k^3/k^6 ratios less than 1.

Even for **3/6a**, the observed ratio of 1.2 is close to unity. These thermodynamic and reactivity trends also held for reactions with the same set of allylic alcohols and olivetol **7** (Table 3, entries 6-10). It should be noted that the key difference in orcinol *vs.* olivetol is the alkyl chain (pentyl *vs.* methyl group); this change did impact the results for obtaining

high ratios of normal to abnormal neocannabinoids. Using orcinol as a reagent, lower yields obtained may be attributed to competition between normal, abnormal, *bis*-addition, and cyclized products. In addition, we found that use of allylic alcohol **10e** led to lower yields of neocannabinoid monoadducts (*cf.* Table 3, entries 3 and 8), largely due to more sluggish reactivity of this partner.

We next hypothesized that an increase in steric bulk on the resorcinol alkyl chain could further drive initial formation of the normal neocannabinoid isomer.[29] This hypothesis led us to evaluate the bulky 5-(1,1-dimethylheptyl) resorcinol partner **7b**. Using this resorcinol partner, we observed formation of the normal neocannabinoid as the major isomer at 1 h with all allylic alcohols employed which we posited was due to increased steric strain imposed by the dimethyl heptyl chain (**3bc-3bf**). DFT calculations also confirmed that the normal isomers were significantly more stable as reaction products and were also kinetically preferred.

Overall, the experimental and computational findings shown in Table 3 support a mechanism that initially produces the abnormal neocannabinoid derivative when there is less steric bulk surrounding the cation intermediate and the normal neocannabinoid in cases of greater steric bulk. This mechanistic correlation can be visualized by the select examples shown in Figure 2 outlining the computed differences in Gibbs free energy of the corresponding abnormal and normal isomer transition states. We also noticed that many transition states leading to both normal and abnormal isomers displayed stabilization imparted by C-H- π interactions[36] (see Supporting Information). Figure 3 shows examples of global minimum transition states highlighting these interactions enroute to normal H_2CBD isomer **3** and abnormal isomer **6**. As shown in Figure 2, the difference in the alkyl chain of products **3ad** and **6ad** *vs.* **3d** and **6d** show that the energy needed to kinetically form abnormal product **6ad** is preferred in comparison to the energy needed to form abnormal isomer **6d**. By leveraging this mechanism and terminating the reaction at different timepoints, we can favor production of either normal or abnormal neocannabinoids based on steric considerations. As previously described, efficient synthesis of abnormal analogues could be a valuable asset in cannabinoid therapeutics; Table 4 highlights examples of abnormal isomers accessed in moderate yields by terminating the reaction at a 1 h timepoint.

As a final study, we sought to test whether the condition-dependent regioselective reactions could also be applied to access neocannabinoids with alternative, unnatural ring sizes for the terpenoid fragment. Accordingly, we synthesized both 5- and 7-member cyclic allylic alcohols **17** and **20**, respectively, and subjected them to the general reaction conditions shown in Scheme 4. These reactions were found to tolerate each ring size wherein both abnormal and normal neocannabinoids were generated and isolated, with *bis*-addition byproducts generated using allylic alcohols **17** and **20**. When tracking these reactions, using orcinol and olivetol we again observed that abnormal products (**18, 18a, 21, 21a**) were produced in competition with the normal isomers (**19, 19a, 22, 22a**) and over time produced more normal isomer due to product equilibration. Use of 5-(1,1,-dimethylheptyl) resorcinol as reaction partner again supported the idea that steric bulk inhibits formation of abnormal products (**18b, 21b**) where only the normal neocannabinoid product was observed with use of both 5- and 7-member cyclic allylic alcohols.

CONCLUSIONS

Herein, we report the synthesis of diverse neocannabinoids using controlled Friedel-Crafts reactions for construction of either the abnormal or normal isomer. We have demonstrated the scope and limitations of this process over 35 examples to produce synthetic unnatural analogs of both normal and abnormal cannabidiol (CBD). Improved understanding of the kinetic and thermodynamic properties for the process can be leveraged in the future towards predictive neocannabinoid synthesis. Moreover, our ongoing and future studies will continue to investigate the power of neocannabinoids as therapeutics and in targeted medicinal chemistry applications which will be the subject of future publications from our laboratories.

Supplementary Material

Refer to Web version on PubMed Central for supplementary material.

ACKNOWLEDGMENTS

The authors thank Dr. Norman Lee of the Boston University Chemical Instrumentation Center for HRMS data and analyses. We thank CBDQure Inc. for funding the initial phases of the project and the National Institutes of Health (NIH) (R35 GM 118173) for additional financial support. We also thank Nick Wangtz (Shanghai Xishite Biosciences Co., Ltc.) for a generous donation of divarinol. We also thank the National Science Foundation (NSF) for support of NMR (CHE-0619339) and MS (CHE-0443618) facilities at Boston University. Computational work reported on in this paper was performed on the Shared Computing Cluster (SCC) which is administered by Boston University's Research Computing Services.

ABBREVIATIONS

CBD	cannabidiol
THC	tetrahydrocannabinol
H_2CBD	8,9-dihydrocannabidiol
Abn-CBD	abnormal cannabidiol, DFT density-functional theory
GPR	G-protein coupled receptor
NMR,	nuclear magnetic resonance
HPCL	high-performance liquid chromatography

REFERENCES

(1). Adams R; Hunt M; Clark JH; Clark JH; Loewe DS Structure of Cannabidiol, a Product Isolated from the Marihuana Extract of Minnesota Wild Hemp. I. J. Am. Chem. Soc 1940, 62, 196–200.

(2). Atalay S; Jarocka-karpowicz I; Skrzydlewskas E Antioxidative and Anti-Inflammatory Properties of Cannabidiol. Antioxidants. 2020, 9, 21.

(3). Pisanti S; Malfitano AM; Ciaglia E; Lamberti A; Ranieri R; Cuomo G; Abate M; Faggiana G; Proto MC; Fiore D; Laezza C; Bifulco M Cannabidiol: State of the Art and New Challenges for Therapeutic Applications. J. Pharm. Thera 2017, 175, 133–150.

(4). Ben-Shabat S; Hanuš LO; Katzavian G; Gallily R New Cannabidiol Derivatives: Synthesis, Binding to Cannabinoid Receptor, and Evaluation of Their Anti-inflammatory Activity. J. Med. Chem 2006, 49, 1113–1117. [PubMed: 16451075]

(5). Nelson KM; Bisson J; Singh G; Graham JG; Chen SN; Friesen JB; Dahlin JL; Niemitz M; Walters MA; Pauli GF The Essential Medicinal Chemistry of Cannabidiol (CBD). J. Med. Chem 2020, 63, 12137–12155. [PubMed: 32804502]

(6). Mascal M; Hafezi N; Wang D; Hu Y; Serra G; Dallas ML; Spencer JPE Synthetic, Non-Intoxicating 8,9-Dihydrocannabidiol for the Mitigation of Seizures. Sci. Rep 2019, 9, 7778. [PubMed: 31123271]

(7). Bloemendal VRLJ; van Hest JCM; Rutjes FPJT Synthetic Pathways to Tetrahydrocannabinol (THC): An Overview. Org. Biomol. Chem 2020, 18, 3203–3215. [PubMed: 32259175]

(8). Leite R; Carlini EA; Lander N; Mechoulam R Anticonvulsant Effects of the (−) and (+) Isomers of Cannabidiol and Their Dimethylheptyl Homologs. Pharmacology. 1982, 24, 141–146. [PubMed: 7071126]

(9). Ashton CJ, The Atypical Cannabinoid O-1602: Targets, Actions, and the Central Nervous System. Cent. Nerv. Syst. Agents. Med. Chem 2012, 12, 233–239. [PubMed: 22831390]

(10). Johns DG; Behm DJ; Walker DJ; Ao Z; Shapland EM; Daniels DA; Riddick M; Dowell S; Staton PC; Green P; Shabon U; Bao W; Aiyar N; Yue TL; Brown AJ; Morrison AD; Douglas SA The Novel Endocannabinoid Receptor GPR55 Is Activated by Atypical Cannabinoids but Does Not Mediate Their Vasodilator Effects. Br. J. Pharmacol 2007, 152, 825–831. [PubMed: 17704827]

(11). Hanuš LO; Meyer SM; Muñoz E; Taglialatela-Scafati O; Appendino G Phytocannabinoids: A Unified Critical Inventory. Nat. Prod. Rep 2016, 33, 1357–1392. [PubMed: 27722705]

(12). Jentsch NG; Zhang X; Magolan J Efficient Synthesis of Cannabigerol, Grifolin, and Piperogalin via Alumina-Promoted Allylation. J. Nat. Prod 2020, 83, 2587–2591. [PubMed: 32972142]

(13). Kearney S; Gangano A; Navaratne P; Barrus D; Rehrauer K; Reid T-E; Roitberg A; Ghiviriga I; Cunningham C; Gamage T; Grenning A Axially Chiral Cannabinoids: Design, Synthesis, and Cannabinoid Receptor Affinity. J. Am. Chem. Soc 2023, 145, 13581–13591. [PubMed: 37314891]

(14). Lago-Fernandez A; Redondo V; Hernandez-Folgado L; Figuerola-Asencio L; Jagerovic N New Methods for the Synthesis of Cannabidiol Derivatives, in: Methods Enzymol., Academic Press Inc 2017, 593, 237–257.

(15). Pirrung MC Synthetic Access to Cannabidiol and Analogs as Active Pharmaceutical Ingredients. J. Med. Chem 2020, 63, 12131–12136. [PubMed: 32531156]

(16). Anand R; Cham PS; Gannedi V; Sharma S; Kumar M; Singh R; Vishwakarma RA; Singh PP Stereoselective Synthesis of Nonpsychotic Natural Cannabidiol and Its Unnatural/Terpenyl/Tail-Modified Analogues. J. Org. Chem 2022, 87, 4489–1498. [PubMed: 35289168]

(17). Grimm JAA; Zhou H; Properzi R; Leutzsch M; Bistoni G; Nienhaus J; List B Catalytic Asymmetric Synthesis of Cannabinoids and Menthol from Neral. Nature. 2023, 615, 634–639. [PubMed: 36859552]

(18). Maiocchi A; Barbieri J; Fasano V; Passarella D Stereoselective Synthetic Strategies to (−)-Cannabidiol. ChemistrySelect. 2022, 7, e202202400.

(19). Baek S-H; Srebnik M; Mechoulam R Boron Triflouride Etherate on Alimina - a Modified Lewis Acid Reagent. Tet. Lett 1985, 26, 1083–1086.

(20). Gaoni Y; Mechoulam R Hashish—VII: The Isomerization of Cannabidiol to Tetrahydrocannabinols. Tetrahedron. 1966, 22, 1481–1488.

(21). Petrzilka T; Haefliger W; Sikemeier C Synthese von Haschisch-Inhaltsstoffen. 4. Mitteilung. Helv. Chim. Acta 1969, 52, 1102–1134.

(22). Bloemendal VRLJ; Spierenburg B; Boltje TJ; van Hest JCM; Rutjes FPJT One-Flow Synthesis of Tetrahydrocannabinol and Cannabidiol Using Homo- and Heterogeneous Lewis Acids. J. Flow. Chem 2021, 11, 99–105.

(23). Crombie L; Crombie WML, Cannabinoid Bis-Homologues: Miniaturised Synthesis and GLC Study. Phytochemistry. 1975, 14, 213–220.

(24). Appendino G; Gibbons S; Giana A; Pagani A; Grassi G; Stavri M; Smith E; Rahman MM Anti-bacterial Cannabinoids from Cannabis Sativa : A Structure–Activity Study. J. Nat. Prod 2008, 71, 1427–1430. [PubMed: 18681481]

(25). Nguyen GN; Jordan EN; Kayser O Synthetic Strategies for Rare Cannabinoids Derived from Cannabis Sativa. J. Nat. Prod 2022, 85, 1555–1568. [PubMed: 35648593]

(26). Kulkarni P. Methane Sulphonic Acid Is Green Catalyst in Organic Synthesis. Orient. J. Chem 2015, 31, 447–451.

(27). Crombie L; Crombie WML; Firth DF Terpenylations Using (R)-(−)-α-Phellandrene. Synthesis of the (3S,4R)-8,9-Dihydro-o- and -p-Cannabidiols, Their Iso-THC's, and the Natural Dihydrochalcone (3S,4R)-(+)-Linderatin. J. Chem. Soc., Perkin Trans. 1 1988, 5, 1251–1253.

(28). Crombie L; Crombie WML; Jamieson SV; Palmer CJ Acid-Catalysed Terpenylations of Olivetol in the Synthesis of Cannabinoids. J. Chem. Soc., Perkin Trans. 1 1988, 5, 1243.

(29). Razdan RK; Dalzell HC; Handrick GR Hashish. X. Simple One-Step Synthesis of (−)-.DELTA. 1-Tetrahydrocannabinol (THC) from p-Mentha-2,8-Dien-1-Ol and Olivetol. J. Am. Chem. Soc 1974, 96, 5860–5865. [PubMed: 4413630]

(30). Iwata T; Kawano R; Fukami T; Shindo M Retro-Friedel-Crafts-Type Acidic Ring-Opening of Triptycenes: A New Synthetic Approach to Acenes. Chem. Eur. J 2022, 28, e202104160. [PubMed: 35015328]

(31). Neese F. The ORCA Program System. Wiley Interdiscip. Rev. Comput. Mol. Sci 2012, 2, 73–78.

(32). Neese F. Software Update: The ORCA Program System, Version 4.0. Wiley Interdiscip. Rev. Comput. Mol. Sci 2018, 8, e1327.

(33). Neese F; Wennmohs F; Becker U; Riplinger C The ORCA Quantum Chemistry Program Package. J. Chem. Phys 2020, 152, 224108. [PubMed: 32534543]

(34). Neese F. Software Update: The ORCA Program System—Version 5.0. WIREs Comput. Mol. Sci 2022, 12, e1606.

(35). Grimme S; Hansen A; Ehlert S; Mewes J-M R2SCAN-3c: A "Swiss Army Knife" Composite Electronic Structure Method. J. Chem. Phys 2021, 154, 064103. [PubMed: 33588555]

(36). Hobza P. Stacking Interactions. Phys. Chem. Chem. Phys 2008, 10, 2581–2583. [PubMed: 18464972]

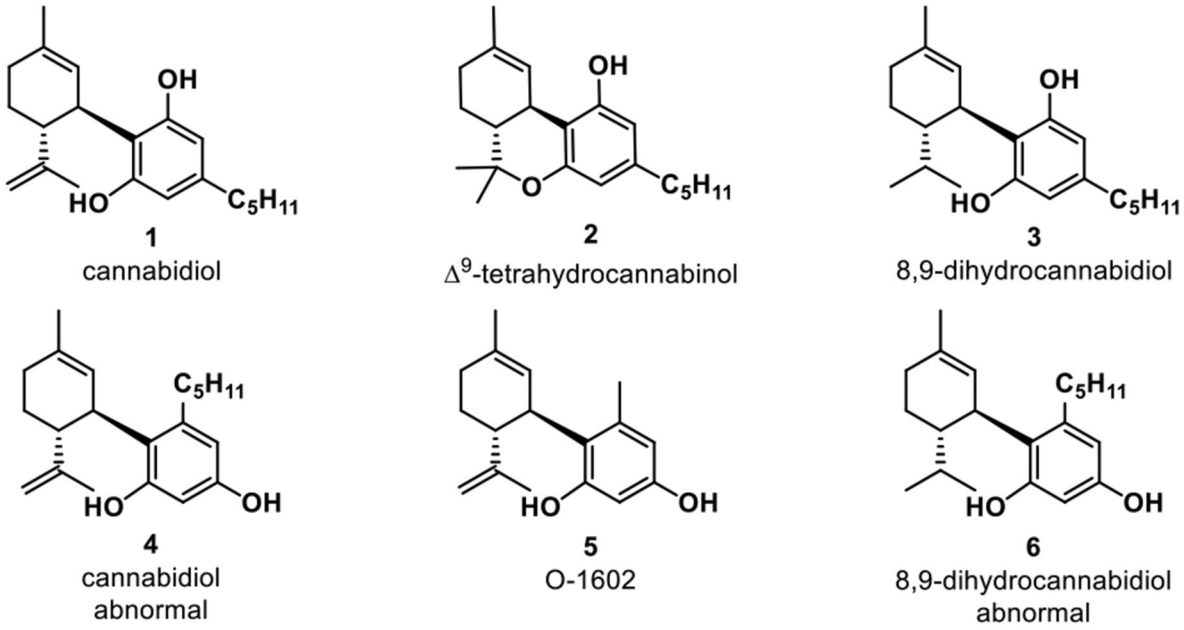

Figure 1.
Natural and synthetic cannabinoids.

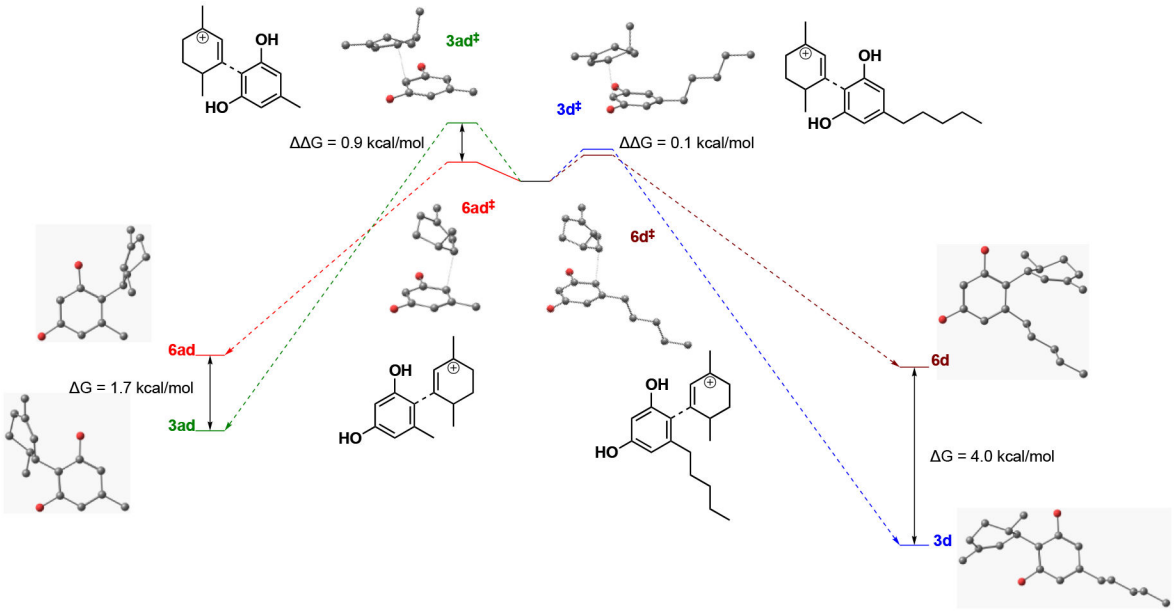

Figure 2.

Qualitative energy diagrams for neocannabinoid isomers **3ad, 6ad, 3d**, and **6d** with the corresponding 3D models. The positions of isomer pairs on the y-axis are a guide for the eyes only and are not meant to represent absolute energies.

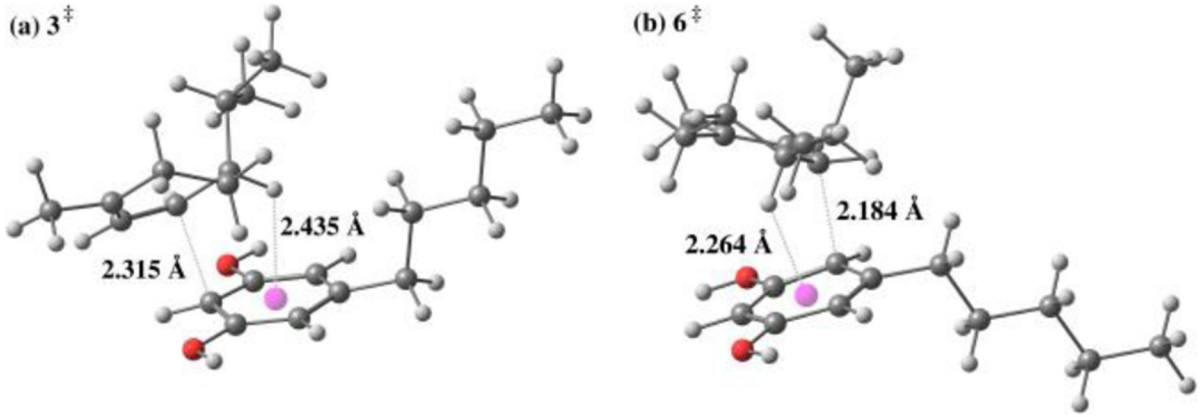

Figure 3.

Global minimum transition state structures for normal (**a, 3**‡) and abnormal (**b, 6**‡) isomers highlighting stabilization imparted by C-H π interactions. The pink sphere is the center of the resorcinol aryl ring.

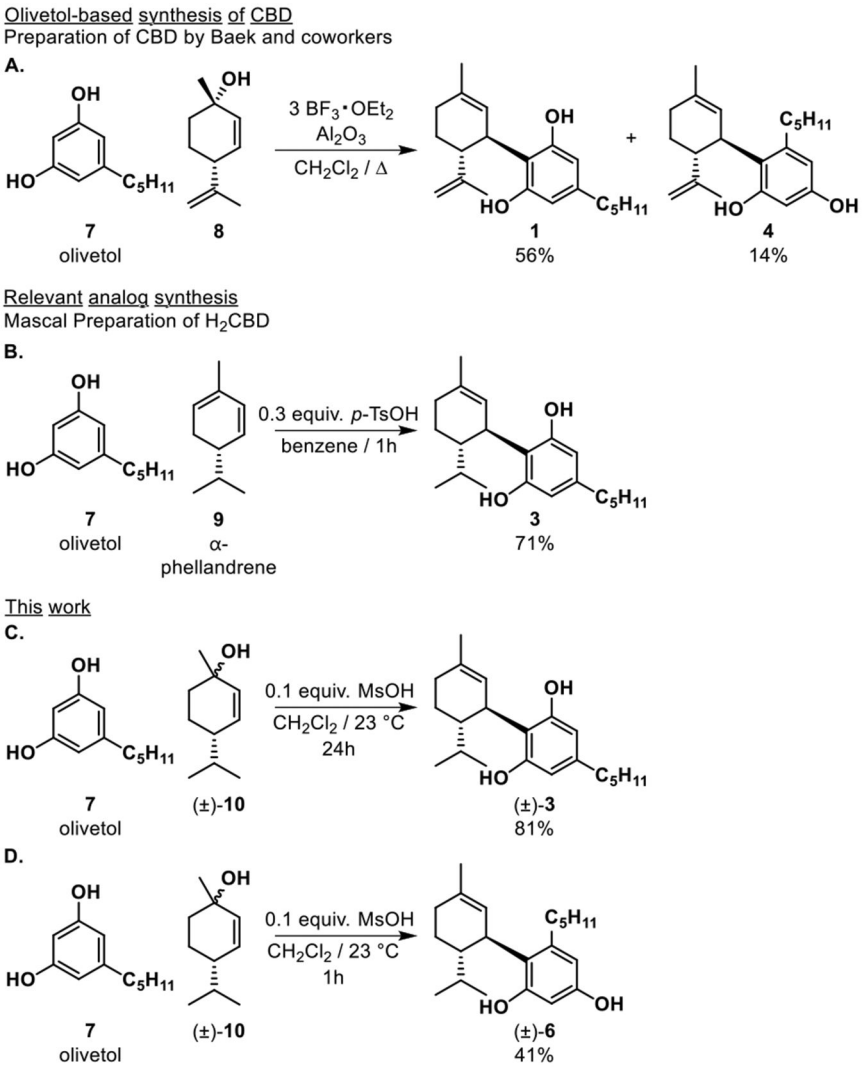

Scheme 1.

Synthesis of CBD isomers and dihydro-CBD regioisomers

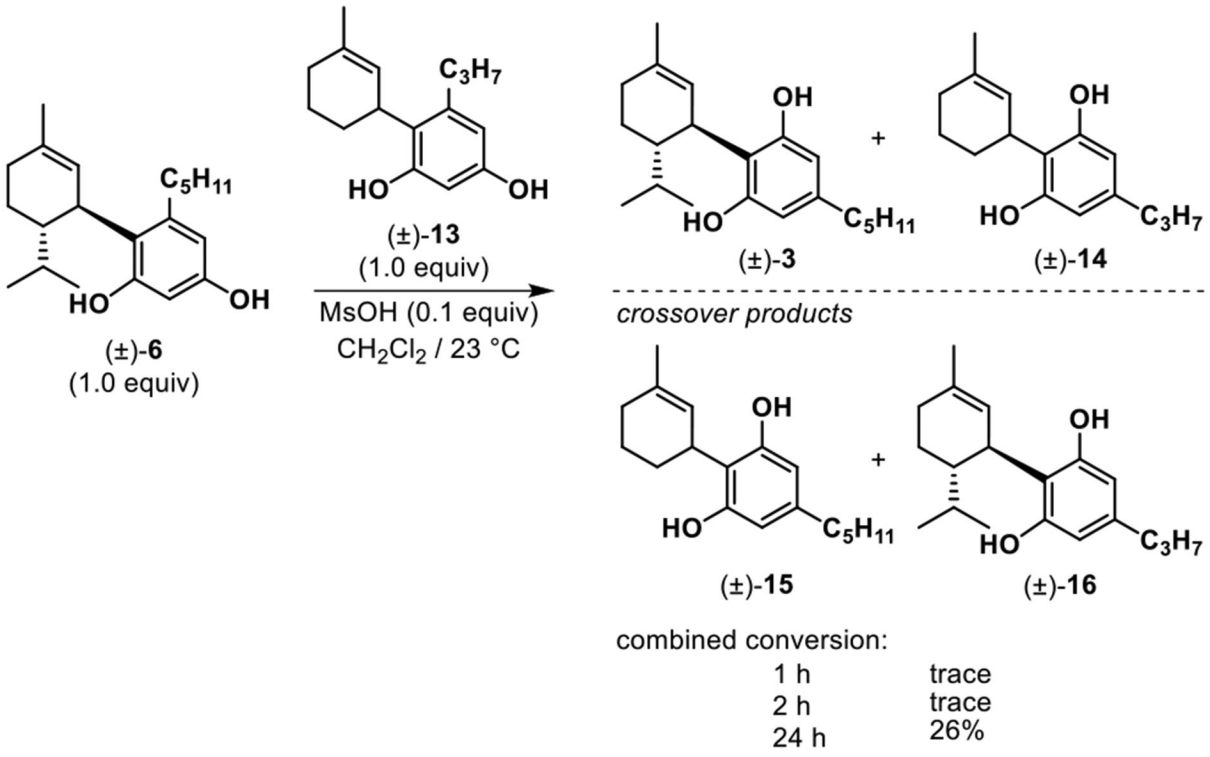

Scheme 2.

Crossover experiment between abnormal cannabinoids 6 and 13 and tracking formation of crossover products

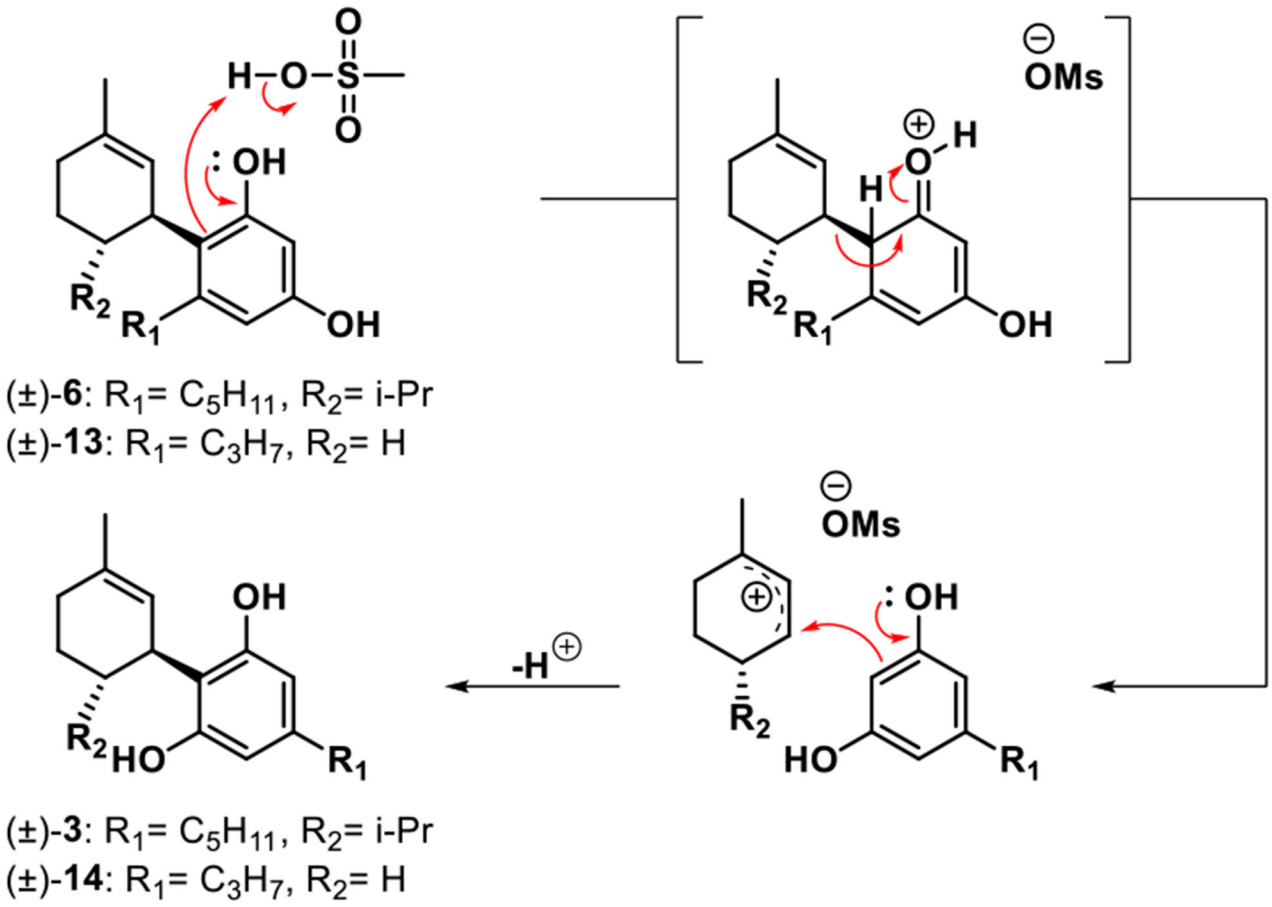

Scheme 3.
Proposed mechanism for equilibration of abnormal to normal neocannabinoids 6 and 13 to 3 and 14

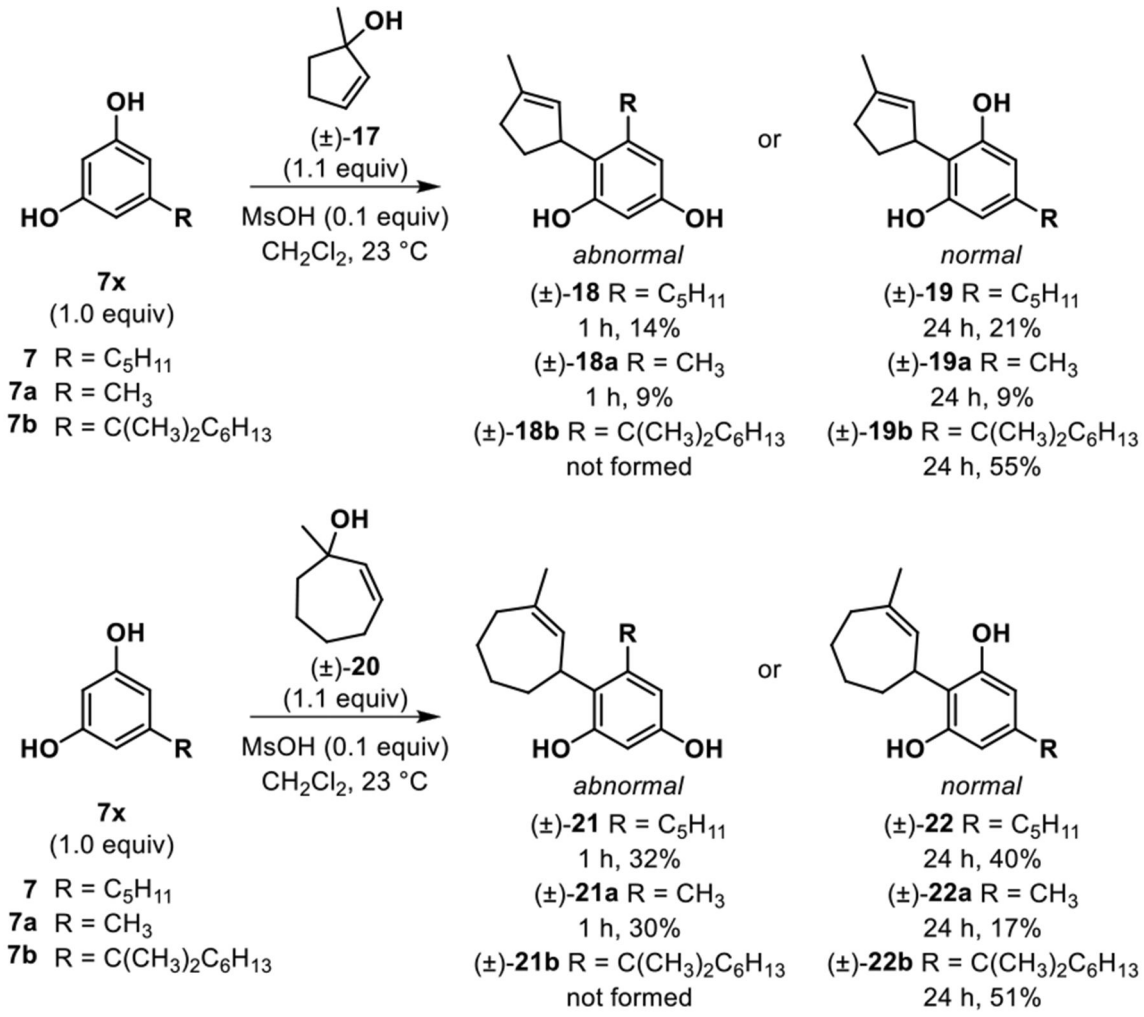

Scheme 4.
Neocannabinoid synthesis from alternate cyclic allylic alcohols

Table 1.

Acid screening scope for Friedel-Crafts reactions

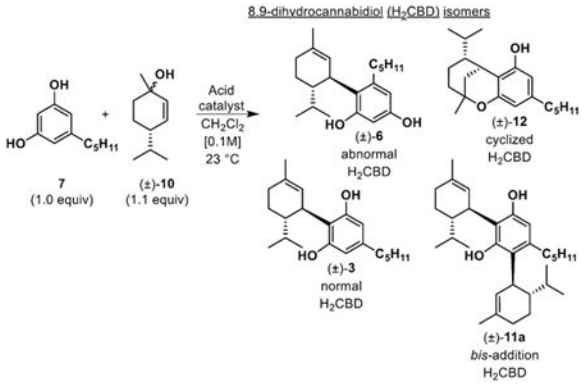

Entry	Acid	Amt.	Time (h)	Conversion[a]	(±)-6[b]	(±)-3[b]
1	$La(OTf)_3$	20 mol%	1	35%	10%	25%
2			24	78%	4%	52%
3	$Yb(OTf)_3$	20 mol%	1	35%	10%	25%
4			24	75%	9%	47%
5	MsOH	10 mol%	1	90%	41%[b]	39%
6			24	99%	0%	81%[b]
7	*p*-TsOH	10 mol%	1	78%	30%	36%
8			24	91%	8%	63%

[a] Conversion measured by ^{1}H NMR analysis.

[b] Isolated yield after silica gel chromatography.

Table 2.

Equilibration of abnormal to normal H_2CBD by *in situ* ^{1}H NMR analysis

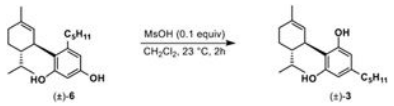

time (h)	(±)-6	(±)-3	(±)-11 and (±)-12
1	40%	60%	0
2	10%	90%	0
6	2%	74%	24%
24	0%	50%	50%

Table 3.

Kinetic *vs.* thermodynamic study of various neocannabinoids with experimental selectivity ratios and DFT-calculated energies

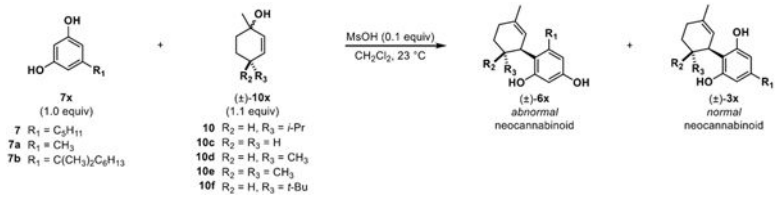

Entry	Resorcinol 7x	Allylic alcohol 10x	(r.r.), 1 h (3x:6x)[a]	(r.r.), 24 h (3x:6x)[a]	Isolated product (±)-3x	% Yield isolated (±)-3x, 24 h	Computational results	
							K^3/k^6 [b]	ΔG (kcal/mol)[c]
1	7a	10c	(1:3)	(1:1)	3ac	9%	0.48	1.3
2	7a	10d	(2:5)	(3:4)	3ad	37%	0.24	1.7
3	7a	10e	(1:10)	(3:10)	3ae	16%	0.48	5.9
4	7a	10	(2:3)	(11:1)	3a	47%	1.20	4.8
5	7a	10f	(5:1)	(9:1)	3af	51%	0.34	4.0
6	7	10c	(7:10)	(1:1)	3c	43%	0.67	1.0
7	7	10d	(1:1)	(5:1)	3d	56%	0.85	4.0
8	7	10e	(1:4)	(1:3)	3e	18%	0.51	2.1
9	7	10	(11:10)	(1:0)	3	81%	0.49	1.7
10	7	10f	(27:1)	(25:1)	3f	75%	2.34	1.7
11	7b	10c	(1:0)	(1:0)	3bc	98%	4.52	7.3
12	7b	10d	(1:0)	(1:0)	3bd	98%	8.80	9.3
13	7b	10e	(1:0)	(1:0)	3be	72%	206.01	11.4
14	7b	10	(1:0)	(1:0)	3b	79%	49.72	10.8
15	7b	10f	(1:0)	(1:0)	3bf	56%	117.65	11.9

[a] Ratio determined by HPLC/ELSD/MS and ^{1}H NMR analysis.

[b] $k^3/k^6 = e^{\Delta\Delta G/kT}$, where ΔΔG = G(6x‡) – G(3x‡), T = 298.15 K, and G(3/6x‡) is the Boltzmann-averaged free energy.

[c] ΔG = G(6x) – G(3x), where G(3/6x) is the Boltzmann-averaged free energy.

Table 4.

Optimized syntheses of abnormal neocannabinoid derivatives

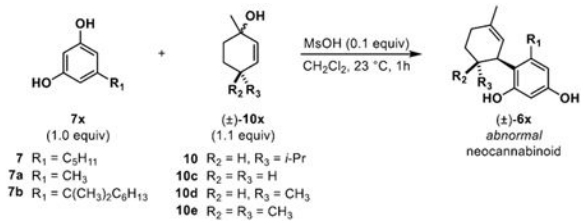

Entry	Resorcinol 7x	Allylic alcohol 10x	Isolated product (±)-6x	% Isolated yield (±)-6x
1	7a	10c	6ac	35%
2	7a	10d	6ad	50%
3	7a	10e	6ae	33%
4	7a	10	6a	40%
5	7	10c	6c	50%
6	7	10d	6d	37%
7	7	10e	6e	24%
8	7	10	6	41%